1 From Infinite Dimensions to Real Materials

Dieter Vollhardt
Center for Electronic Correlations and Magnetism
University of Augsburg

Contents

E. Pavarini, E. Koch, A. Lichtenstein, and D. Vollhardt (eds.)
DMFT: From Infinite Dimensions to Real Materials
Modeling and Simulation Vol. 8
Forschungszentrum Jülich, 2018, ISBN 978-3-95806-313-6
http://www.cond-mat.de/events/correl18

1 From materials to models

In view of the great complexity of nature, scientific explanations of natural phenomena can only be found by appropriate simplifications, namely through idealization and abstraction ("reduction"). This requires modelling. Models are supposed to take into account the most important features of a complicated object or process, neglecting features which are considered less important. This has been an extremely successful approach in science, especially in physics. Take, for example, a steam engine in a power plant. Many aspects of the functional principle of such a large and technically complicated machine can already be understood in terms of a simple mechanical model consisting of a cylinder and piston, and using the concept of temperature, pressure, and volume. For a long time mechanical models were thought to be indispensable for an understanding of physical phenomena. Indeed, in 1861 Maxwell, the founding father of the highly elegant theory of electromagnetism, introduced a mechanical model of electromagnetism [1] based on vortices in a molecular medium, which looks rather bizarre to us today. Although it helped Maxwell to explain the displacement current, the molecular vortex model did not turn out to be useful to understand electromagnetism and was soon abandoned. This shows that models have to prove their usefulness over the course of time – otherwise they will be discarded.

1.1 The long way to a model for ferromagnetism in 3d transition metals

When it comes to materials and the explanation of their properties the question again arises what kind of models to use. One of the most famous properties of solids which is known for a very long time already [2] is ferromagnetism, in particular in magnetite (Fe_3O_4) and elemental iron (Fe). What is a good model to understand ferromagnetism? A crucial step in the development of a microscopic theory of ferromagnetism in solids was the model of magnetic domains proposed by Weiss [3] in 1906, where he postulated the alignment of elementary magnets due to the existence of a "molecular field", also referred to as "Weiss mean field". But what is the origin of this peculiar field?

Starting from the interaction between neighboring elementary magnets the Ising model [4] was formulated almost 20 years later to provide a microscopic explanation of the molecular field. Ising solved the one-dimensional problem, found that a phase transition does not occur, and concluded (incorrectly) that this was also the case in three dimensions. The Ising model is a classical spin model. Earlier it had been shown by Bohr (1911) and van Leeuwen (1919) that magnetism is actually a quantum effect. Therefore another important step in the development of a theory of ferromagnetism was Heisenberg's formulation of a quantum spin model in 1928 [5]. The Heisenberg model explains the Weiss molecular field as the result of a quantum mechanical exchange process. But this model includes only the spin degree of electrons, i.e., describes localized electrons.

In 1929 Bloch [6] pointed out that such a model cannot explain ferromagnetism as observed in 3d transition metals such as iron, cobalt and nickel, and that an appropriate model had to

include the *itineracy* of the electrons, i.e., their wave nature, which in a solid leads to electronic bands. However, the conditions for ferromagnetism which he obtained for free electrons where unrealistic.[1] Obviously one has to go beyond free electrons and take also their mutual *interaction* into account. This immediately leads to an enormously difficult many-body problem, which is made especially complicated by the fermionic nature of the electrons, their long-range Coulomb interaction, their high density in the metallic state, and the presence of a periodic lattice potential. Attempts by Slater [8] in 1936 to explain ferromagnetism in Ni by including the Coulomb interaction within Hartree-Fock theory were not successful. In particular, the screening of the bare Coulomb repulsion was a difficult issue. It became clear that one had to include genuine correlation effects within well-defined approximations.[2] This implies two intimately connected problems: the formulation of a sufficiently simple model of correlated electrons which unifies the competing approaches by Heisenberg and Bloch (namely the picture of localized and itinerant electrons, respectively), and its solution within more or less controlled approximations. Progress in this direction was slow. One reason certainly was that in the nineteen-thirties and forties nuclear physics attracted more attention than solid-state physics, with a very specific focus of research during the 2nd World War. But apart from that, the sheer complexity of the many-body problem itself did not allow for quick successes. High hurdles had to be overcome, both regarding the development of appropriate mathematical techniques (field-theoretic and diagrammatic methods, Green functions, etc.) and physical concepts (multiple scattering, screening of the long-range Coulomb interaction, quasiparticles and Fermi liquid theory, electron-phonon coupling, superconductivity, metal-insulator transitions, disorder, super-exchange, localized magnetic states in metals, etc.).[3]

At the Washington Conference on Magnetism, held at the University of Maryland on September 2-6, 1952, the conceptual problems regarding a theory of ferromagnetism in $3d$ transition metals were discussed in detail. This resulted in a series of articles in the Reviews of Modern Physics, including papers by Slater [11], Wohlfarth [12], and van Vleck [13], which summarized the understanding of this fundamental problem at that time. But in spite of great progress in many areas of condensed matter physics a microscopic model for metallic ferromagnetism, or of interacting electrons in general, did not emerge until 1963, when a model for correlated lattice electrons was proposed independently by Gutzwiller [14], Hubbard [15], and Kanamori [16]. All three wanted to explain ferromagnetism in $3d$ transition metals. This model is now called "Hubbard model" and is the fundamental theoretical model for electronic correlations in solids.

[1] For a historical review of the development of the quantum-mechanical theory of metals from 1928 to 1933, which describes the conceptual problems of that time, see Ref. [7].

[2] Apparently Wigner [9] was the first who tried to calculate the contribution of the mutual electronic interaction to the ground state energy relative to the Hartree-Fock result, which he called "correlation energy".

[3] A discussion of the many-body problem and of some of the important developments up to 1961 can be found in the lecture notes and reprint volume by Pines [10].

1.2 Electronic correlations

The concept of electronic correlations plays a very important role in modern condensed matter physics. It refers to electronic interaction effects which cannot be explained within a static mean-field picture and which therefore go beyond results obtained by factorization approximations such as Hartree or Hartree-Fock mean-field theory. Correlation effects are particularly strong in materials with partially filled d and f electron shells and narrow energy bands, as in the $3d$ transition metals or the rare–earths and their compounds.
Electronic correlations in solids lead to the emergence of complex behavior, resulting in rich phase diagrams. In particular, the interplay between the spin, charge, and orbital degrees of freedom of the correlated d and f electrons with the lattice degrees of freedom leads to a cornucopia of correlation and ordering phenomena including heavy fermion behavior [17], high temperature superconductivity [18], colossal magnetoresistance [19], Mott metal-insulator transitions [20], and Fermi liquid instabilities [21]. Such properties are not only of interest for fundamental research but also have a great potential for technological applications. Namely, the great sensitivity of correlated electron materials with respect to changes of external parameters such as temperature, pressure, electromagnetic fields, and doping can be employed to develop materials with useful functionalities [22]. Consequently there is a great need for the development of appropriate models and theoretical investigation techniques which allow for a comprehensive, and at the same time reliable, exploration of correlated electron materials [23–25].

1.3 The Hubbard model

The single-band Hubbard model [14–16] is the simplest microscopic lattice model for interacting electrons in a solid such as $3d$ electrons in transition metals [26]. The Hamiltonian consists of two terms, the kinetic energy $\hat{H}_0$ and the interaction energy $\hat{H}_{\rm int}$ (in the following operators are denoted by a hat):

$$\hat{H} = \hat{H}_0 + \hat{H}_{\rm int} \tag{1a}$$

$$\hat{H}_0 = \sum_{\boldsymbol{R}_i,\boldsymbol{R}_j}\sum_{\sigma} t_{ij}\,\hat{c}^\dagger_{i\sigma}\hat{c}_{j\sigma} = \sum_{\boldsymbol{k},\sigma}\varepsilon_{\boldsymbol{k}}\hat{n}_{\boldsymbol{k}\sigma} \tag{1b}$$

$$\hat{H}_{\rm int} = U\sum_{\boldsymbol{R}_i}\hat{n}_{i\uparrow}\hat{n}_{i\downarrow} \equiv U\hat{D}. \tag{1c}$$

Here $\hat{c}^\dagger_{i\sigma}(\hat{c}_{i\sigma})$ are creation (annihilation) operators of fermions with spin σ at site $\boldsymbol{R}_i$ (for simplicity denoted by i), $\hat{n}_{i\sigma} = \hat{c}^\dagger_{i\sigma}\hat{c}_{i\sigma}$, and $\hat{D}$ is the operator of total double occupation of the lattice sites. The Fourier transform of the kinetic energy in (1b), where t_{ij} is the amplitude for hopping between sites i and j, involves the dispersion $\varepsilon_{\boldsymbol{k}}$ and the momentum distribution operator $\hat{n}_{\boldsymbol{k}\sigma}$. A schematic picture of the Hubbard model is shown in Fig. 1.
In the Hubbard model the Coulomb interaction between two electrons is assumed to be so strongly screened that it can be described as a purely local interaction which occurs only *on* a

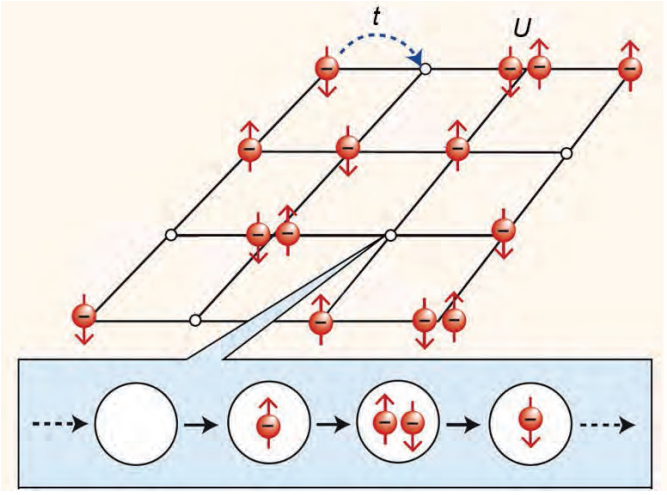

Fig. 1: *Schematic illustration of interacting electrons in a solid described by the Hubbard model. The ions enter only as a rigid lattice, here represented by a square lattice. The electrons, which have mass, negative charge, and spin (↑ or ↓), are quantum particles which move from one lattice site to the next with a hopping amplitude t. Together with the lattice structure this determines the band structure of the non-interacting electrons. The quantum dynamics leads to fluctuations in the occupation of lattice sites as indicated by the sequence: a lattice site can either be unoccupied, singly occupied (↑ or ↓), or doubly occupied. When two electrons meet on a lattice site, which is only possible if they have opposite spin because of the Pauli exclusion principle, they encounter a local interaction U.*

lattice site.[4] In view of the Pauli principle the interaction is therefore only possible if the two electrons have opposite spin. A direct interaction between electrons with equal spin direction, e.g., on neighboring sites, is not described by the model, but can be easily included. The interaction is therefore completely independent of the lattice structure and spatial dimension of the system. This property distinguishes it from other model interactions since it has no classical counterpart. The kinetic energy $\hat{H}_0$ is diagonal in momentum space and reflects the wave nature of the electrons, while the interaction energy $\hat{H}_{\rm int}$ is diagonal in position space and characterizes their particle nature.

The physics described by the Hubbard model is clearly very different from that of bare electrons with a long-range Coulomb interaction. Therefore the Hubbard model is far from obvious. Its formulation required fundamentally new insights as explained in section 1.1. In particular, screening is a basic ingredient of the many-body problem of metals.

As discussed above, the Hubbard model was originally introduced to provide a microscopic explanation of ferromagnetism in $3d$ transition metals [14–16]. How should this model be able to do that? In fact, the interaction energy is lowest (zero) when double occupation of lattice sites is fully suppressed, i.e., when the spins of electrons are ferromagnetically aligned. From the point of view of the interaction alone one can therefore expect the ground state to be ferromagnetic for sufficiently strong repulsion U. However, this argument neglects the kinetic

[4] In particular, the Hubbard model applies to lattice fermions with a point interaction, such as cold atoms in optical lattices where the bare interaction is indeed extremely short-ranged [27, 28]; see section 5.2.2.

energy. While the lattice structure and spatial dimension do not affect the Hubbard interaction at all, they play a very important role for the kinetic energy since they determine the structure of the density of states of the non-interacting electrons. This is especially important for the stabilization of ferromagnetism and will be discussed in more detail in section 6.1.
In spite of the extreme simplifications made by the Hubbard model in comparison with interacting electrons in a real solid, it still cannot be solved analytically, except in dimension $d = 1$ for nearest-neighbor hopping [29]. For dimensions $d = 2, 3$, approximations are required.[5] Here "mean-field theories" play a particularly important role.

2 Mean-field theories

In the statistical theory of classical and quantum-mechanical systems a rough, overall description of the properties of a model can often be obtained within a mean-field theory. While in the full many-body model a particle or spin experiences a complicated, fluctuating field generated by the other particles or spins, in a mean-field theory this fluctuating field is approximated by an average ("mean") field. Usually, but not always, the full interaction problem then reduces to an effective, single-particle problem — a self-consistent field theory.
A mean-field theory can often be constructed by letting some variable or parameter become large (in fact, infinite), whereby fluctuations are suppressed. Depending on the model this can be the length of the spins S, the spin degeneracy N, the spatial dimension d, or the coordination number Z, i.e., the number of nearest neighbors of a lattice site.[6] Mean-field theories obtained in such a limit, supplemented if possible by an expansion in the inverse of the large parameter, can provide valuable insights into the fundamental properties of a model. Perhaps the best-known mean-field theory in many-body physics is the Weiss molecular-field theory for the Ising model [31]. It is a prototypical "single-site mean-field theory" which becomes exact in the limit of infinite coordination number Z or infinite dimensions d.

2.1 Infinite dimensions

The meaning of "infinite dimensions" needs some explanation. Already in $d = 3$ the coordination number can be quite large, e.g., $Z = 6$ for a simple cubic lattice, $Z = 8$ for a bcc lattice and $Z = 12$ for an fcc-lattice, making its inverse, $1/Z$, rather small. It is then interesting to investigate whether the limit $Z \to \infty$ leads to some simplifications. For a hypercubic lattice, obtained by generalizing the simple cubic lattice in $d = 3$ to arbitrary dimensions, one has $Z = 2d$. The limit $d \to \infty$ is then equivalent to $Z \to \infty$.

[5] In view of the complexity of the many-body problem in condensed matter theory, progress in this field relies on making good approximations. As Peierls wrote: "*... the art of choosing a suitable approximation, of checking its consistency and finding at least intuitive reasons for expecting the approximation to be satisfactory, is much more subtle than that of solving an equation exactly*" [30].

[6] For regular lattices both a dimension d and a coordination number Z can be defined. The coordination number Z is then determined by the dimension d and the lattice structure. But there exist other lattice-like structures, such as the Bethe lattice, which cannot be associated with a physical dimension d, although a coordination number Z is well-defined.

It is interesting to note that investigations in statistical mechanics based on the simplifications arising in the limit of infinite coordination number Z or dimension d do not go far back. In fact, Z originally denoted the number of spins in the *range* of the interaction [32]. In this case the limit $Z \to \infty$ describes an infinitely long-ranged interaction.[7] Since a particle or spin at a given site then interacts with infinitely many other particles or spins (which are all "neighbors"), this limit was referred to as "limit of infinite dimensions" or "limit of high density" [32]. It was found that the Weiss mean-field theory for the Ising model becomes exact in this limit. Starting with Fisher and Gaunt [33] in 1964 the Ising model and other classical models were investigated on general d-dimensional simple hypercubic lattices. Now Z is really the coordination number, i.e., the number of nearest neighbors, as we use it today, with $Z = 2d$. For the Ising model the limit of infinitely long-ranged spin coupling J and the limit of infinite dimensions d both yield the same result, namely the Weiss mean-field theory.

2.2 Weiss mean-field theory for the Ising model

The Hamiltonian for the Ising model with nearest-neighbor coupling between two classical spins is given by

$$H = -\frac{1}{2} J \sum_{\langle \boldsymbol{R}_i, \boldsymbol{R}_j \rangle} S_i S_j \,, \tag{2}$$

where we assume ferromagnetic coupling ($J > 0$) and summation over nearest-neighbor sites. This can also be written as

$$H = \sum_{\boldsymbol{R}_i} h_i S_i \,, \tag{3}$$

where now every spin S_i interacts with a local field

$$h_i = -J \sum_{\boldsymbol{R}_j}^{(i)} S_j \tag{4}$$

produced by the spins on nearest-neighbor sites; here the superscript (i) implies summation over the nearest-neighbor sites of $\boldsymbol{R}_i$. In the Weiss mean-field theory the spin interaction in (2), or the interaction of a spin with the local field in (3), are decoupled, i.e., H is replaced by a mean-field Hamiltonian

$$H^{\mathrm{MF}} = h_{\mathrm{MF}} \sum_{\boldsymbol{R}_i} S_i + E_{\mathrm{shift}} \,. \tag{5}$$

Now a spin S_i interacts only with a global ("molecular") field

$$h_{\mathrm{MF}} \equiv \langle h_i \rangle = -JZS \,, \tag{6}$$

[7] This limit can be even used in one-dimensional particle models, in which case the equation of state reduces to the van der Waals equation [31].

where $\langle\ \rangle$ indicates the thermal average, $\langle S_i\rangle \equiv S$, $E_{\rm shift} = \frac{1}{2}\ LJZ\langle S\rangle^2$ is a constant energy shift, and L is the number of lattice sites. Formally this result can be obtained by employing the factorization

$$\big\langle (S_i - S)(S_j - S)\big\rangle = 0\,, \tag{7}$$

whereby correlated fluctuations of spins at sites $\boldsymbol{R}_i$ and $\boldsymbol{R}_j$ are neglected. In the limit $Z \to \infty$ the coupling constant J needs to be rescaled as

$$J \to \frac{J^*}{Z}\,,\ J^* = \text{const} \tag{8}$$

for $h_{\rm MF}$, and thereby the energy, to remain finite. In this limit the factorization (7), and hence the replacement of (2) by the mean-field Hamiltonian (5), becomes exact [32, 34]. Eq. (5) implies that in the limit $Z \to \infty$ fluctuations of a finite number of spins in the "bath" of surrounding neighbors become unimportant, such that the surrounding of any site is completely described by a single mean-field $h_{\rm MF}$. Hence the Hamiltonian becomes purely local

$$H^{\rm MF} = \sum_{\boldsymbol{R}_i} H_i + E_{\rm shift}\,, \tag{9}$$

where $H_i = h_{\rm MF} S_i$. Thereby the problem reduces to an effective single-site problem. The value of S (the "magnetization") is determined by the self-consistent Curie-Weiss or Bragg-Williams equation

$$S = \tanh(\beta J^* S), \tag{10}$$

where $\beta = 1/(k_B T)$ and the self-consistency condition (6) was used. The scaling (8) is typical for localized spin models.

The Weiss mean-field theory is seen to become exact in the limit of infinite coordination number Z or dimension d. In this case $1/Z$ or $1/d$ serve as a small parameter which can be used to improve the mean-field theory systematically. The Weiss mean-field theory contains no unphysical singularities, is applicable for all values of the input parameters (temperature and/or additional external magnetic field), and is diagrammatically controlled [35]. Therefore it is often viewed as a prototypical mean-field theory in statistical mechanics.

2.3 Hartree mean-field theory for the Hubbard model

Lattice fermion models such as the Hubbard model are much more complicated than localized spin models. Therefore the construction of a mean-field theory with the comprehensive properties of the Weiss mean-field theory for the Ising model will be more complicated, too.

The simplest static mean-field theory for the Hubbard model is the Hartree approximation [36–38]. To clarify the shortcomings of this mean-field theory we proceed as in the derivation of the Weiss mean-field theory for the Ising model and factorize the interaction term. To this end we rewrite the Hubbard interaction in the form of (3), i.e., we let an electron with spin σ at site $\boldsymbol{R}_i$ interact with a local field $\hat{h}_{i\sigma}$ produced by an electron with opposite spin on that site[8]

[8] This field is described by an operator and therefore has a dynamics.

$$\hat{H}_{\rm int} = \sum_{\boldsymbol{R}_i} \sum_{\sigma} \hat{h}_{i\sigma} \hat{n}_{i\sigma}, \tag{11}$$

where $\hat{h}_{i\sigma} = \frac{1}{2} U \hat{n}_{i-\sigma}$. As in the derivation of the Weiss mean-field theory we now factorize the two-particle interaction in (11), i.e., we replace $\hat{H}$ by

$$\hat{H}^{\rm MF} = \hat{H}_{\rm kin} + \sum_{\boldsymbol{R}_i, \sigma} \langle \hat{h}_{i\sigma} \rangle \hat{n}_{i\sigma} + E_{\rm shift} \, . \tag{12}$$

Now a σ-electron at site $\boldsymbol{R}_i$ interacts only with a local, *static* field (a c-number)

$$\langle \hat{h}_{i\sigma} \rangle = \frac{1}{2} U n_{-\sigma} \, , \tag{13}$$

where $n_{-\sigma} = \langle \hat{n}_{i-\sigma} \rangle$ is the global density of $(-\sigma)$-electrons. The above decoupling of the operators corresponds to the Hartree approximation,[9] which assumes

$$\big\langle (\hat{n}_{i\sigma} - n_\sigma)(\hat{n}_{i-\sigma} - n_{-\sigma}) \big\rangle = 0, \tag{14}$$

whereby correlated fluctuations *on* the site $\boldsymbol{R}_i$ are neglected.

It is important to note that although (12) is now a one-particle problem it still cannot be solved exactly, since, in principle, the potential (the static mean field $\langle \hat{h}_{i\sigma} \rangle$) may vary from site to site. This is a new feature due to the quantum-mechanical kinetic energy, which enters as an additional term in the Hamiltonian.

The Hartree approximation becomes exact in the weak-coupling limit ($U \to 0$) and/or the low-density limit ($n \to 0$). But how about $d \to \infty$? Does it become exact in this limit for all input parameters (temperature, density, interaction strength)? The answer is clearly no: the Hubbard interaction is purely local and hence independent of the spatial dimensions. Although the factorizations (7) and (14) are mathematical identical, the physics they imply is very different. Namely, (7) describes the decoupling of a spin from a bath of infinitely many neighboring spins in which fluctuations do indeed become unimportant in the limit $d \to \infty$, while (14) corresponds to the decoupling of an electron from *one* other electron (with opposite spin) on the same site. For strong repulsion U double occupation of a lattice site is energetically unfavorable and is therefore suppressed. In this situation the local correlation function $\langle \hat{n}_{i\uparrow} \hat{n}_{i\downarrow} \rangle$ must not be factorized, since otherwise correlation phenomena are immediately eliminated. It is therefore clear that the Hartree decoupling, which factorizes the local quantum dynamics, can never become exact in any dimension or for any coordination number, since $\langle \hat{n}_{i\uparrow} \hat{n}_{i\downarrow} \rangle \neq \langle \hat{n}_{i\uparrow} \rangle \langle \hat{n}_{i\downarrow} \rangle$, unless $U \to 0$ and/or $n \to 0$. Hence the nature of the Hartree mean-field theory for spin-$\frac{1}{2}$ electrons with on-site interaction is very different from the Weiss mean-field theory for spins with nearest-neighbor coupling.

[9] Since the Hubbard interaction acts only between electrons with opposite spin on the same lattice site an exchange (Fock) term does not arise.

3 Gutzwiller variational method

Another useful but very different approximation scheme for quantum many-body systems, which has a long and successful history in theoretical many-body physics [39], makes use of variational wave functions. Starting from a many-body trial wave function the energy expectation value is calculated and then minimized with respect to physically motivated variational parameters. Although variational wave functions usually yield only approximate results, they have several advantages: they are physically intuitive, can be custom tailored to a particular problem, and can be used even when standard perturbation methods fail or are inapplicable.
For the analytic investigation of the electronic correlation model which Gutzwiller [14] had introduced (and which was later named after Hubbard), he had also proposed a very simple variational wave function. This "Gutzwiller wave function" introduces correlations into the wave function for non-interacting particles via a purely local correlation factor in real space, which is constructed from the double occupation operator $\hat{D}$ as

$$|\,\Psi_G\rangle \;=\; g^{\hat{D}}\,|\mathrm{FG}\rangle \tag{15a}$$

$$\;=\; \prod_{\boldsymbol{R}_i}\big(1-(1-g)\hat{D}_i\big)|\mathrm{FG}\rangle. \tag{15b}$$

Here $|\mathrm{FG}\rangle$ is the wave function of non-interacting fermions (Fermi Gas), g is a variational parameter with $0 \le g \le 1$, and $\hat{D}_i = \hat{n}_{i\uparrow}\hat{n}_{i\downarrow}$ is the operator of double occupation of lattice site $\boldsymbol{R}_i$, which monitors the interaction on that site. The projector $g^{\hat{D}}$ globally reduces the amplitude of those spin configurations in $|\mathrm{FG}\rangle$ which have too many doubly occupied sites for given repulsion U. The limit $g = 1$ describes the non-interacting case, while $g \to 0$ corresponds to strong coupling (usually $U \to \infty$). The Gutzwiller wave function can be used to calculate the expectation value of an operator, e.g., the ground state energy $\bar{E}(g,U)$ of the Hubbard model, using the Hamiltonian (1). By computing the minimum of $\bar{E}(g,U)$, the variational parameter g is determined as a function of the interaction parameter U.

3.1 Gutzwiller approximation

In general the evaluation of expectation values cannot be performed exactly. Therefore Gutzwiller introduced a non-perturbative approximation scheme which allowed him to obtain an explicit expression for the ground state energy of the Hubbard model [14, 40]; for details see Refs. [41, 24]. The Gutzwiller approximation is based on the counting of classical spin configurations and is therefore a quasiclassical approximation. The idea behind the approximation can be illustrated by calculating the norm $\langle\Psi_G|\Psi_G\rangle$. In configuration space the ground state of the Fermi gas can be written as

$$|\mathrm{FG}\rangle = \sum_D \sum_{\{i_D\}} A_{i_D}|\Psi_{i_D}\rangle, \tag{16}$$

where $|\Psi_{i_D}\rangle$ is a spin configuration with D doubly occupied sites and A_{i_D} is the corresponding probability amplitude. The sum extends over the whole set $\{i_D\}$ of different configurations with

the same D, and over all D. For a system with L lattice sites and N_σ σ-electrons the number N_D of different configurations in $\{i_D\}$ is given by the combinatorial expression

$$N_D = \frac{L!}{L_\uparrow!\, L_\downarrow!\, D!\, E!}\,, \tag{17}$$

where $L_\sigma = N_\sigma - D$, and $E = L - N_\uparrow - N_\downarrow + D$ are the numbers of singly occupied and empty sites, respectively. Since $|\Psi_{i_D}\rangle$ is an eigenstate of $\hat{D}$, the norm of $|\Psi_G\rangle$ reads

$$\langle\Psi_G|\Psi_G\rangle = \sum_D g^{2D} \sum_{\{i_D\}} |A_{i_D}|^2. \tag{18}$$

In the Gutzwiller approximation spatial correlations between the spins of the electrons are neglected. The probability $|A_{i_D}|^2$ is then the same for all configurations of electrons on the lattice, i.e., is given by the classical combinatorial result for uncorrelated particles

$$|A_{i_D}|^2 = P_\uparrow P_\downarrow, \tag{19}$$

where $P_\sigma = 1/\binom{L}{N_\sigma} = N_\sigma!\,(L - N_\sigma)!/L! \simeq n_\sigma^{N_\sigma}(1 - n_\sigma)^{L-N_\sigma}$, with $n_\sigma = N_\sigma/L$, is the probability for an arbitrary configuration of σ-electrons. In this case (18) reduces to

$$\langle\Psi_G|\Psi_G\rangle = P_\uparrow P_\downarrow \sum_D g^{2D} N_D. \tag{20}$$

In the thermodynamic limit the sum in (20) is dominated by its largest term corresponding to a value $D = \bar{D}$, where $\bar{D}$ is determined by

$$g^2 = \frac{\bar{d}\,(1 - n_\uparrow - n_\downarrow + \bar{d})}{(n_\downarrow - \bar{d})(n_\uparrow - \bar{d})}\,, \tag{21}$$

where $\bar{d} = \bar{D}/L$. Eq. (21) has the form of the law of mass action, where the correlation parameter g^2 rather than the Boltzmann factor regulates the dynamical equilibrium between the concentrations of singly occupied sites on one side of this "chemical reaction" and that of doubly occupied sites and holes on the other.[10] The calculation of the expectation values of the kinetic and the interaction energy of the Hubbard model proceeds similarly [41]. We will later see that the Gutzwiller approximation leads to the correct results for the expectation value of an operator calculated in terms of the Gutzwiller wave function in the limit $d = \infty$.

3.2 Brinkman-Rice transition

The results of the Gutzwiller approximation [14,40] describe a correlated, normal-state fermionic system at zero temperature whose momentum distribution has a discontinuity q at the Fermi level, with $q = 1$ in the non-interacting case, which is reduced to $q < 1$ by the interaction as in a Landau Fermi liquid. In 1970 Brinkman and Rice [43] observed that in the case of a half-filled

[10] In fact, eq. (21), with g^2 replaced by the Boltzmann factor $e^{-\beta U}$, is the exact result for the Hubbard model with infinite-range hopping [42].

band ($n_\uparrow = n_\downarrow = 1/2$) the Gutzwiller approximation describes a transition at a finite critical interaction strength U_c from an itinerant to a localized state, where lattice sites are singly occupied and the discontinuity q vanishes. This "Brinkman-Rice transition" therefore corresponds to a correlation induced (Mott) metal-insulator transition. They argued [43] that the inverse of q can be identified with the effective mass of Landau quasiparticles, $q^{-1} = m^*/m \geq 1$, which diverges at U_c.

The results obtained with the Gutzwiller approximation are physically very reasonable. In fact, in the nineteen-seventies and eighties it was the only approximation scheme which was able to describe a Mott metal-insulator transition at a finite value of the interaction *and* was in accord with basic properties of Landau Fermi liquid theory.[11] This was confirmed by a detailed investigation of the assumptions and implications of the Gutzwiller approximation which I published in 1984 [41], and in which I showed that the Gutzwiller-Brinkman-Rice theory was not only in qualitative [46], but even in good quantitative agreement with experimentally measured properties of normal-liquid ^{3}He; for a discussion see section 3 in Ref. [47].

3.3 Systematic derivation of the Gutzwiller approximation?

The results of the Gutzwiller approximation are clearly mean-field-like since, for example, the kinetic energy of the correlated system is obtained by renormalizing the kinetic energy of non-interacting single-particle states $(\boldsymbol{k}, \sigma)$ by an overall factor q. This is also one of the reasons why the results obtained for the Hubbard lattice model have a much wider range of applicability, i.e., can even be used to understand liquid ^{3}He [41, 48]. However, the validity of the Gutzwiller approximation was still unclear in 1984. In particular, it was not known how to improve this approximation — after all it was based on the calculation of *quantum-mechanical* matrix elements from the most probable *classical* spin configurations. The question was, whether the Gutzwiller approximation could be derived in a controlled way, for example by calculating expectation values of operators with the Gutzwiller wave function using quantum many-body perturbation theory in a well-defined limit, or by some other method of quantum many-body theory. This question was answered a few years later, when the Gutzwiller approximation was re-derived in two different ways: as a slave-boson mean-field theory [49][12] and in the limit of infinite spatial dimensions [52], as will be discussed below.

[11] Other well-known approximation schemes, in particular those proposed by Hubbard, did not have these important properties: in the Hubbard-I approximation [15], which interpolates between the atomic limit and the non-interacting band, a band gap exists for any $U > 0$ (so there is no Mott transition at all), while the Hubbard-III approximation [44] corresponds to the coherent potential approximation [45] for disordered systems, in which case the Fermi surface volume is not conserved.

[12] Kotliar and Ruckenstein [50] formulated a functional integral representation of the Hubbard and Anderson models in terms of auxiliary bosons, whose simplest saddle-point approximation ("slave-boson mean-field theory") reproduces exactly the results of the Gutzwiller approximation [49]. Thus they showed that the results of the Gutzwiller approximation can also be obtained without the use of the Gutzwiller variational wave function.

4 Lattice fermions in infinite dimensions

The expectation values of the kinetic and the interaction energy of the Hubbard model (1) in terms of the Gutzwiller wave function can, in principle, be calculated within diagrammatic many-body perturbation theory for arbitrary dimensions d. Introducing a new analytic approach in which the expectation values were expressed by sums over different lattice sites, Walter Metzner and I showed that these calculations can be greatly simplified [51, 52].[13] Thereby we were able to calculate the diagrams analytically to all orders in $d = 1$, which led to analytic results for the ground-state energy for arbitrary density n and interaction strength U [51, 52].[14] In $d > 1$ analytic calculations to all orders were not possible. But by evaluating individual diagrams numerically in dimensions as high as $d = 15$ we observed that in $d = \infty$ the values of these diagrams could equally be obtained if momentum conservation at a vertex was neglected, i.e., if the momenta carried by the lines of a diagram were assumed to be independent. When summed over all diagrams this approximation gave exactly the results of the Gutzwiller approximation [52]. Thus the Gutzwiller approximation had been derived systematically within quantum many-body perturbation theory in the limit of infinite spatial dimensions. Apparently the limit $d \to \infty$ was not only useful for the investigation of spin models, but also for fermions.

4.1 Simplifications of diagrammatic many-body perturbation theory

The simplifications of the diagrammatic many-body perturbation theory in the limit $d \to \infty$ are due to a collapse of irreducible diagrams, which implies that only local diagrams remain [57, 58]. In particular, the irreducible self-energy is then completely local (Fig. 2). To understand this diagrammatic collapse let us consider diagrams where lines correspond to one-particle density matrices, $g^0_{ij,\sigma}$, as they enter in the calculation of expectation values with the Gutzwiller wave function (nevertheless the following arguments are equally valid for the one-particle Green function $G^0_{ij,\sigma}(\omega)$[15]). The one-particle density matrix may be interpreted as the amplitude for transitions between sites $\boldsymbol{R}_i$ and $\boldsymbol{R}_j$. The square of its absolute value is therefore proportional to the *probability* for a particle to hop from $\boldsymbol{R}_j$ to a site $\boldsymbol{R}_i$. In the case of nearest-neighbor sites on a lattice with coordination number Z this implies $|g^0_{ij,\sigma}|^2 \sim \mathcal{O}(1/Z)$. For nearest-neighbor

[13] The resulting diagrams have the same form as Feynman diagrams in many-body perturbation theory (due to the locality of the interaction they are identical to those of a Φ^4 theory), but a line corresponds to a one-particle density matrix $g^0_{ij,\sigma} = \langle \hat{c}^\dagger_{i\sigma} \hat{c}_{j\sigma} \rangle_0$ and not to a one-particle propagator $G^0_{ij,\sigma}(\omega)$ since in the variational approach there is no dynamics.

[14] Correlation functions can also be calculated analytically in $d = 1$ [53, 54] and provide further insights into the properties of the Gutzwiller wave function. For example, the result for the spin–spin correlation function show that in the strong coupling limit the Gutzwiller wave function describes spin correlations in the nearest-neighbor, isotropic Heisenberg chain extremely well and coincides with the exact solution of the spin-1/2 antiferromagnetic Heisenberg chain with an exchange interaction falling off as $1/r^2$ [55, 56]; for a discussion see section 4.1 in Ref. [47].

[15] This follows directly from $g^0_{ij,\sigma} = \lim_{t \to 0^-} G^0_{ij,\sigma}(t)$ and the fact that the scaling properties do not depend on the time evolution and the quantum-mechanical representation. The Fourier transform of $G^0_{ij,\sigma}(\omega)$ also preserves this property. For this reason the same results as those obtained in the calculation with the Gutzwiller wave function hold: all connected one-particle irreducible diagrams collapse in position space, i.e., are purely diagonal in $d = \infty$.

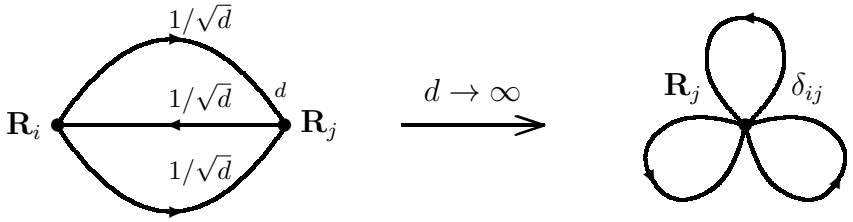

Fig. 2: *Collapse of the irreducible self-energy diagram for the Hubbard model in second-order perturbation theory in U in the limit $d \to \infty$.*

sites $\boldsymbol{R}_i$ and $\boldsymbol{R}_j$ on a hypercubic lattice (where $Z = 2d$) one therefore finds for large d [57, 58]

$$g^0_{ij,\sigma} \sim \mathcal{O}\left(\frac{1}{\sqrt{d}}\right). \tag{22}$$

For general i, j one obtains [58, 59]

$$g^0_{ij,\sigma} \sim \mathcal{O}\left(1/d^{\|\boldsymbol{R}_i - \boldsymbol{R}_j\|/2}\right). \tag{23}$$

Here $\| \boldsymbol{R} \| = \sum_{n=1}^{d} |R_n|$ is the length of $\boldsymbol{R}$ in the "New York metric", where particles only hop along horizontal or vertical lines, never along a diagonal; for further discussions of diagrammatic simplifications see Ref. [60].[16]

For non-interacting electrons at $T = 0$ the expectation value of the kinetic energy is given by

$$E^0_{\rm kin} = -t \sum_{\langle \boldsymbol{R}_i, \boldsymbol{R}_j \rangle} \sum_{\sigma} g^0_{ij,\sigma}\,. \tag{24}$$

On a hypercubic lattice the sum over nearest neighbors leads to a factor $\mathcal{O}(d)$. In view of the $1/\sqrt{d}$ dependence of $g^0_{ij,\sigma}$ it is therefore necessary to scale the nearest-neighbor hopping amplitude t as

$$t \to \frac{t^*}{\sqrt{d}}\,, \quad t^* = \text{const.}, \tag{25}$$

since only then the kinetic energy remains finite for $d \to \infty$. The same result is obtained in a momentum-space formulation.[17] It is important to bear in mind that, although $g^0_{ij,\sigma} \sim 1/\sqrt{d}$

[16] Gebhard [61] showed that it is possible to calculate with the Gutzwiller wave function in the limit $d = \infty$ even without diagrams. Thereby he re-derived the full set of static saddle-point equations of the slave-boson approach and provided a direct connection between the slave-boson mean-field theory [49] and the diagrammatic calculation of expectation values in terms of the Gutzwiller wave function in $d = \infty$ [57, 58]. The approach was generalized by him and collaborators to multi-band Hubbard models into a "Gutzwiller density functional theory" which can be used to describe the effect of correlations in real materials [62, 63].

[17] This can be seen by calculating the density of states of non-interacting particles. For nearest-neighbor hopping on a d-dimensional hypercubic lattice $\varepsilon_{\boldsymbol{k}}$ has the form $\varepsilon_{\boldsymbol{k}} = -2t \sum_{i=1}^{d} \cos k_i$ (here and in the following we set Planck's constant $\hbar$, Boltzmann's constant k_B, and the lattice spacing equal to unity). The density of states corresponding to $\varepsilon_{\boldsymbol{k}}$ is given by $N_d(\omega) = \sum_{\boldsymbol{k}} \delta(\omega - \varepsilon_{\boldsymbol{k}})$, which is the probability density for finding the value $\omega = \varepsilon_{\boldsymbol{k}}$ for a random choice of $\boldsymbol{k} = (k_1, \ldots, k_d)$. If the momenta k_i are chosen randomly, $\varepsilon_{\boldsymbol{k}}$ is the sum of d many independent (random) numbers $-2t \cos k_i$. The central limit theorem then implies that in the limit $d \to \infty$ the density of states is given by a Gaussian, i.e., $N_d(\omega) \stackrel{d\to\infty}{\longrightarrow} \frac{1}{2t\sqrt{\pi d}} \exp\left[-\left(\frac{\omega}{2t\sqrt{d}}\right)^2\right]$. Only if t is scaled with d as in (25) does one obtain a non-trivial density of states $N_\infty(\omega)$ in $d = \infty$ [38, 57] and thus a finite kinetic energy.

vanishes for $d \to \infty$, the particles are not localized, but are still mobile. Indeed, even in the limit $d \to \infty$ the off-diagonal elements of $g^0_{ij,\sigma}$ contribute, since particles may hop to d many nearest neighbors with amplitude $t^*/\sqrt{d}$.
A rescaling of the microscopic parameters of the Hubbard model with d is only required in the kinetic energy, since the interaction term is independent of the spatial dimension. Altogether this implies that only the Hubbard Hamiltonian with a rescaled kinetic energy

$$\hat{H} = -\frac{t^*}{\sqrt{d}} \sum_{\langle \boldsymbol{R}_i, \boldsymbol{R}_j \rangle} \sum_{\sigma} \hat{c}^\dagger_{i\sigma} \hat{c}_{j\sigma} + U \sum_{\boldsymbol{R}_i} \hat{n}_{i\uparrow} \hat{n}_{i\downarrow} \tag{26}$$

has a non-trivial $d \to \infty$ limit where both the kinetic energy and the interaction contribute equally. Namely, it is the *competition* between the two terms which leads to interesting many-body physics.

4.1.1 Is there a unique $d \to \infty$ limit for the Hubbard model?

The motivation for the scaling discussed above deserves a more detailed discussion: To obtain a physically meaningful mean-field theory for a model, its internal or free energy has to remain finite in the limit d or $Z \to \infty$. While for the Ising model the scaling $J \to J^*/Z$, J^*= const., is rather obvious, this is not so for more complicated models. Namely, fermionic or bosonic many-particle systems are usually described by a Hamiltonian with several non-commuting terms, e.g., a kinetic energy and an interaction, each of which is associated with a coupling parameter, usually a hopping amplitude and an interaction, respectively. In such a case the question of how to scale these parameters has no unique answer since this depends on the physical effects one wishes to explore. The scaling should be performed such that the model remains non-trivial and that its internal or free energy stays finite in the $d, Z \to \infty$ limit. Here "non-trivial" means that not only $\langle \hat{H}_0 \rangle$ and $\langle \hat{H}_{\rm int} \rangle$ but also the *competition*, expressed by $\langle [\hat{H}_0, \hat{H}_{\rm int}] \rangle$, should remain finite. In the case of the Hubbard model it would be possible to scale the hopping amplitude as in the Weiss mean-field theory, i.e., $t \to t^*/Z,\ t^* = \text{const.}$, but then the kinetic energy would be reduced to zero in the limit $d, Z \to \infty$, making the resulting model uninteresting (but not unphysical) for most purposes. For the bosonic Hubbard model the situation is even more subtle, since the kinetic energy has to be scaled differently depending on whether it describes the normal or the Bose-Einstein condensed fraction; for a discussion see Ref. [64]. Hence, in the case of a many-body system described by a Hamiltonian with several terms, the solution in the limit $d \to \infty$ depends on the scaling of the model parameters.

4.2 The Hubbard model in $d = \infty$

In our 1989 paper [57] Walter Metzner and I had shown (i) that the diagrammatic collapse of diagrams which occurs in the limit $d \to \infty$ leads to great simplifications in quantum many-body perturbation theory and (ii) that the Hubbard model, when scaled properly, stills describes nontrivial correlations among the fermions. This is already apparent from the evaluation of the second-order diagram in Goldstone perturbation theory for the correlation energy at weak

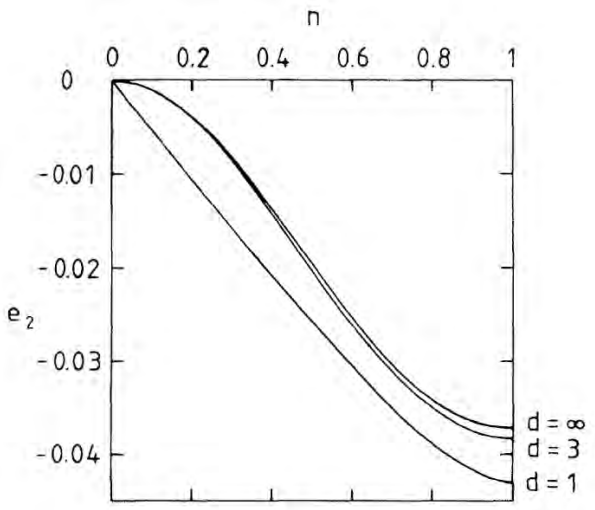

Fig. 3: *Correlation energy of the Hubbard model in second-order Goldstone perturbation theory in U (in units of $2U^2/|\varepsilon_0|$) vs. density n for dimensions $d = 1, 3, \infty$. Here ε_0 is the kinetic energy for $U = 0$ and $n = 1$; adapted from Ref. [57].*

coupling [57]. Namely, the nine-dimensional integral in $d = 3$ over the three internal momenta reduces to a single integral in $d = \infty$, implying that in $d = \infty$ the calculation is simpler than in any other dimension. More importantly, the numerical results obtained in $d = \infty$ turn out to be very close to those in $d = 3$ and therefore provide a computationally simple, but quantitatively reliable approximation (Fig. 3).

These results clearly showed that microscopic calculations for correlated lattice fermions in $d = \infty$ dimensions were useful and very promising. Further insights followed quickly:

(i) Müller-Hartmann [65] proved that in infinite dimensions only local interactions remain dynamical, that the proper self-energy becomes momentum independent[18]

$$\Sigma_\sigma(\boldsymbol{k}, \omega) \overset{d\to\infty}{\equiv} \Sigma_\sigma(\omega), \tag{27}$$

and that therefore typical Fermi liquid features are preserved [66] (for a discussion see section 4.2.3),

(ii) Schweitzer and Czycholl [71] demonstrated that calculations for the periodic Anderson model also become much simpler in high dimensions, and

(iii) Brandt and Mielsch [72] derived the exact solution of the Falicov-Kimball model for infinite dimensions by mapping the lattice problem onto a solvable atomic problem in a generalized,

[18] This result may be understood as follows [67, 68]: The interaction between particles influences their motion. This effect is described by a complex, spatially dependent, and dynamical field — the self-energy $\Sigma_\sigma(\boldsymbol{k}, \omega)$. When a lattice has a very large number of nearest neighbors the *spatial* dependence of this field becomes increasingly unimportant and vanishes completely in $d = \infty$, as in the Weiss mean-field theory. So the field becomes a *mean field* in position space but retains its full dynamics. In this respect there is a direct analogy to non-interacting electrons in the present of static ("quenched") disorder, where the self-energy also becomes purely local ($\boldsymbol{k}$ independent) in the limit $d \to \infty$ ("coherent potential"). The coherent potential approximation [45] is a single-site theory where a particle moves through an effective medium described by the self-energy $\Sigma_\sigma(\omega)$ and becomes exact in $d = \infty$ [69, 70]. It should be noted that the coherent potential in the case of the Hubbard model in the limit $d \to \infty$ is more complicated due to the interaction between the particles (see section 5.1).

time-dependent external field.[19] They also indicated that such a mapping was, in principle, also possible for the Hubbard model.
Due to the property (27) the most important obstacle for diagrammatic calculations in finite dimensions $d \geq 1$, namely the integration over intermediate momenta, is removed. At the same time the limit $d \to \infty$ does not affect the *dynamics* of the system. Hence, in spite of the simplifications in position or momentum space, the many-electron problem retains its full dynamics in $d = \infty$.

4.2.1 Interactions beyond the on-site interaction

In the case of more general interactions than the Hubbard interaction, e.g., nearest-neighbor interactions such as

$$\hat{H}_{nn} = \sum_{\langle \boldsymbol{R}_i, \boldsymbol{R}_j \rangle} \sum_{\sigma\sigma'} V_{\sigma\sigma'}\, \hat{n}_{i\sigma} \hat{n}_{j\sigma'} \tag{28}$$

the interaction constant has to be scaled, too, in the limit $d \to \infty$. Since (28) has the form of a classical interaction, the scaling known from the Ising model

$$V_{\sigma\sigma'} \to \frac{V^*_{\sigma\sigma'}}{Z} \tag{29}$$

is required [65]. Therefore in the limit $d \to \infty$ non-local contributions reduce to their Hartree equivalent and only the Hubbard interaction remains dynamical, as discussed in section 2.3.

4.2.2 One-particle propagator

Due to the $\boldsymbol{k}$-independence of the irreducible self-energy, (27), the one-particle propagator of an interacting lattice fermion system ("lattice Green function") is given by

$$G_{\boldsymbol{k},\sigma}(\omega) = \frac{1}{\omega - \varepsilon_{\boldsymbol{k}} + \mu - \Sigma_\sigma(\omega)}\,. \tag{30}$$

We note that the $\boldsymbol{k}$-dependence of $G_{\boldsymbol{k}}(\omega)$ comes entirely from the energy dispersion $\varepsilon_{\boldsymbol{k}}$ of the *non*-interacting particles. This means that in a homogeneous system described by the propagator

$$G_{ij,\sigma}(\omega) = L^{-1} \sum_{\boldsymbol{k}} G_{\boldsymbol{k},\sigma}(\omega)\, e^{i\boldsymbol{k}\cdot(\boldsymbol{R}_i - \boldsymbol{R}_j)} \tag{31}$$

its local part, $G_{ii,\sigma} \equiv G_\sigma$, is given by

$$G_\sigma(\omega) \;=\; L^{-1} \sum_{\boldsymbol{k}} G_{\boldsymbol{k},\sigma}(\omega) = \int_{-\infty}^{\infty} d\varepsilon\, \frac{N_0(\varepsilon)}{\omega - \varepsilon + \mu - \Sigma_\sigma(\omega)}\,, \tag{32}$$

where $N_0(\varepsilon)$ is the density of states of the non-interacting system. In the paramagnetic phase we can suppress the spin index. The spectral function of the interacting system (also often called density of states) is then given by

$$A(\omega) = -\frac{1}{\pi} \mathrm{Im}\, G(\omega + i0^+). \tag{33}$$

[19] Alternatively, it can be shown that in the limit $Z \to \infty$ the dynamics of the Falicov-Kimball model reduces to that of a non-interacting, tight-binding model on a Bethe lattice with coordination number $Z = 3$ which can thus be solved analytically [73].

4.2.3 Consequences of the k-independence of the self-energy: Fermi liquid behavior

The $\boldsymbol{k}$-independence of the self-energy allows one to make contact with Fermi liquid theory [66]. At $T = 0$ the one-particle propagator (30) takes the form

$$G_{\boldsymbol{k}}(\omega) = \frac{1}{\omega - \varepsilon_{\boldsymbol{k}} + E_F - \Sigma(\omega)}\,. \tag{34}$$

In general, i.e., even when Σ has a $\boldsymbol{k}$-dependence, the Fermi surface is defined by the $\omega = 0$ limit of the denominator of (34)

$$\varepsilon_{\boldsymbol{k}} + \Sigma_{\boldsymbol{k}}(0) = E_F\,. \tag{35a}$$

According to Luttinger and Ward [74] the volume within the Fermi surface is not changed by interactions, provided the latter can be treated in perturbation theory. This is expressed by

$$n = \sum_{\boldsymbol{k}\sigma} \Theta\big(E_F - \varepsilon_{\boldsymbol{k}} - \Sigma_{\boldsymbol{k}}(0)\big), \tag{35b}$$

where n is the particle density and $\Theta(x)$ is the step function. The $\boldsymbol{k}$-dependence of $\Sigma_{\boldsymbol{k}}(0)$ in (35a) implies that, in spite of (35b), the shape of the Fermi surface of the interacting system will be quite different from that of the non-interacting system (except for the rotationally invariant case $\varepsilon_{\boldsymbol{k}} = f(|\boldsymbol{k}|)$. By contrast, for lattice fermion models in $d = \infty$, where $\Sigma_{\boldsymbol{k}}(\omega) \equiv \Sigma(\omega)$, the Fermi surface itself, and hence the enclosed volume, is not changed by the interaction. The Fermi energy is simply shifted uniformly from its non-interacting value E_F^0 to $E_F = E_F^0 + \Sigma(0)$, to keep n in (35b) constant. Thus $G(0)$, the $\omega = 0$ value of the local lattice Green function, and of the spectral function $A(0) = -\frac{1}{\pi}\mathrm{Im}\, G(i0^+)$ are not changed by the interaction at all. This "pinning behavior" is well-known from the single-impurity Anderson model [75]. A renormalization of $N(0)$ can only come from a $\boldsymbol{k}$-dependence of Σ.
For $\omega \to 0$ the self-energy has the property [66]

$$\mathrm{Im}\ \Sigma(\omega) \propto \omega^2, \tag{35c}$$

which implies Fermi liquid behavior. The effective mass of the quasiparticles

$$\frac{m^*}{m} = 1 - \left.\frac{d\Sigma}{d\omega}\right|_{\omega=0} \tag{35d}$$

$$= 1 + \frac{1}{\pi}\int_{-\infty}^{\infty} d\omega\, \frac{\mathrm{Im}\,\Sigma(\omega + i0^-)}{\omega^2} \geq 1 \tag{35e}$$

is seen to be enhanced. In particular, the momentum distribution

$$n_{\boldsymbol{k}} = \frac{1}{\pi}\int_{-\infty}^{0} d\omega\, \mathrm{Im}\, G_{\boldsymbol{k}}(\omega) \tag{36}$$

has a discontinuity at the Fermi surface, given by $n_{k_F^-} - n_{k_F^+} = (m^*/m)^{-1}$, where $k_F^\pm = k_F \pm 0^+$.

5 Dynamical mean-field theory (DMFT)

The diagrammatic simplifications of many-body perturbation theory in infinite spatial dimensions provide the basis for the construction of a comprehensive mean-field theory for lattice fermions which is diagrammatically controlled and whose free energy has no unphysical singularities. The construction is based on the scaled Hamiltonian (26). The self-energy is then momentum independent, but retains its frequency dependence and thereby describes the full many-body dynamics of the interacting system.[20] The resulting theory is mean-field-like *and* dynamical and hence represents a *dynamical mean-field theory* (DMFT) for lattice fermions, which is able to describe genuine correlation effects as will be discussed next.

5.1 The self-consistent DMFT equations

The DMFT equations were derived in 1991/92 by Janiš [67] and Georges and Kotliar [76] in different ways: (i) as a generalization of the coherent potential approximation [67],[21] and (ii) by mapping the lattice electron problem onto a single-impurity Anderson model with a self-consistency condition [76]; the latter mapping was also employed by Jarrell [77]. For a detailed discussion of the two derivations see Ref. [60]. Both derivations make use of the fact that in $d = \infty$ lattice fermion models with a local interaction effectively reduce to a single site embedded in a dynamical mean field provided by the other fermions as illustrated in Fig. 4. Although the DMFT equations derived within the coherent potential approximation approach and by the mapping onto a self-consistent single-impurity Anderson model, respectively, are identical, the latter approach was immediately adopted by the community since it connects with the well-studied theory of quantum impurities and the Kondo problem [75], for whose solution efficient numerical codes such as the quantum Monte-Carlo (QMC) method [78] had already been developed and were readily available. For this reason the single-impurity based derivation of the DMFT immediately became the standard approach. For a detailed derivation see the review by Georges, Kotliar, Krauth, and Rozenberg [79]; an introductory presentation can be found in Ref. [80]. The foundations of the DMFT will be discussed at this Autumn School in the lecture by M. Kollar.

The self-consistent DMFT equations are given by

(I) the *local propagator* $G_\sigma(i\omega_n)$, which is expressed by a functional integral as

$$G_\sigma(i\omega_n) = -\frac{1}{\mathcal{Z}} \int \prod_\sigma \mathcal{D}c_\sigma^* \mathcal{D}c_\sigma \; c_\sigma(i\omega_n)\, c_\sigma^*(i\omega_n) \; \exp(-S_{\rm loc}) \tag{37}$$

with the partition function

$$\mathcal{Z} = \int \prod_\sigma \mathcal{D}c_\sigma^* \mathcal{D}c_\sigma \; \exp(-S_{\rm loc}) \tag{38}$$

[20] This is in contrast to Hartree(-Fock) theory where the self-energy is merely a static potential.

[21] In the coherent potential approximation quenched disorder acting on non-interacting electrons is averaged and produces a mean field, the "coherent potential". For the Hubbard model in $d = \infty$ the infinitely many fluctuating fields generated by the Hubbard-Stratonovich transformation of the Hubbard interaction represent "annealed" disorder acting on non-interacting electrons which, after averaging, produces a mean field, the self-energy [68].

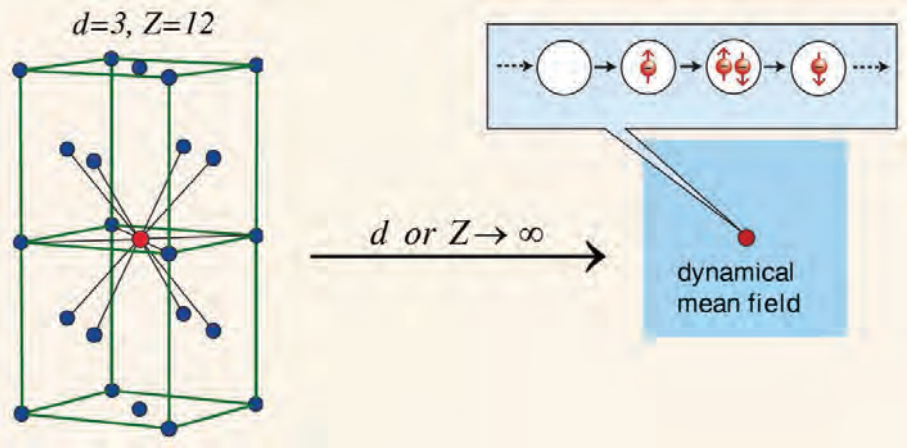

Fig. 4: *In the limit d or $Z \to \infty$ the Hubbard model effectively reduces to a dynamical single-site problem which may be viewed as a lattice site embedded in a $\boldsymbol{k}$-independent, dynamical fermionic mean field. Electrons can hop from the mean field onto this site and back, and interact on the site as in the original Hubbard model (see Fig. 1). The local propagator (i.e., the return amplitude) and the dynamical mean field are the most important quantities in this limit.*

and the local action

$$S_{\rm loc} \;=\; -\int_0^\beta d\tau_1 \int_0^\beta d\tau_2 \sum_\sigma c^*_\sigma(\tau_1)\, \mathcal{G}^{-1}_\sigma(\tau_1 - \tau_2)\, c_\sigma(\tau_2) \;+\; U \int_0^\beta d\tau\, c^*_\uparrow(\tau) c_\uparrow(\tau) c^*_\downarrow(\tau) c_\downarrow(\tau)\,. \quad (39)$$

Here $\mathcal{G}_\sigma$ is the effective local propagator (also called "bath Green function", or "Weiss mean field")[22] which is defined by a Dyson equation

$$\mathcal{G}_\sigma(i\omega_n) = \Big(\big(G_\sigma(i\omega_n)\big)^{-1} + \Sigma_\sigma(i\omega_n) \Big)^{-1}. \quad (40)$$

Furthermore, by identifying the local propagator (37) with the Hilbert transform of the lattice Green function

$$G_{\boldsymbol{k}\sigma}(i\omega_n) = \frac{1}{i\omega_n - \varepsilon_{\boldsymbol{k}} + \mu - \Sigma_\sigma(i\omega_n)} \quad (41)$$

(which is exact in $d = \infty$ [79]) one obtains
(II) the *self-consistency condition*

$$G_\sigma(i\omega_n) = \frac{1}{L}\sum_{\boldsymbol{k}} G_{\boldsymbol{k}\sigma}(i\omega_n) = \int_{-\infty}^{\infty} d\varepsilon\, \frac{N(\varepsilon)}{i\omega_n - \varepsilon + \mu - \Sigma_\sigma(i\omega_n)} \quad (42)$$

$$= \quad G^0_\sigma\big(i\omega_n - \Sigma_\sigma(i\omega_n)\big). \quad (43)$$

In (42) the ionic lattice enters only through the density of states of the non-interacting electrons. Eq. (43) illustrates the mean-field character of the DMFT equations particularly clearly: the local Green function of the interacting system is given by the non-interacting Green function G^0_σ at the renormalized energy $i\omega_n - \Sigma_\sigma(i\omega_n)$, which corresponds to the energy measured relative to the mean-field energy $\Sigma_\sigma(i\omega_n)$ of the surrounding dynamical fermionic bath.

[22] In principle, both the local functions $\mathcal{G}_\sigma(i\omega_n)$ and $\Sigma_\sigma(i\omega_n)$ can be viewed as a dynamical mean field since both appear in the bilinear term of the local action (39).

5.1.1 Solution of the self-consistent DMFT equations

The self-consistent DMFT equations can be solved iteratively: starting with an initial guess for the self-energy $\Sigma_\sigma(i\omega_n)$ one obtains the local propagator $G_\sigma(i\omega_n)$ from (42) and thereby the bath Green function $\mathcal{G}_\sigma(i\omega_n)$ from (40). This determines the local action (39) which is needed to compute a new value for the local propagator $G_\sigma(i\omega_n)$ from (37). By employing the old self-energy a new bath Green function $\mathcal{G}_\sigma$ is calculated and so on, until convergence is reached. It should be stressed that although the DMFT corresponds to an effectively local problem, the propagator $G_{\boldsymbol{k}}(\omega)$ *does* depend on the crystal momentum $\boldsymbol{k}$ through the dispersion relation $\varepsilon_{\boldsymbol{k}}$ of the non-interacting electrons. But there is no additional momentum-dependence through the self-energy, since this quantity is local within the DMFT.
Solutions of the self-consistent DMFT equations require the extensive application of numerical methods, in particular quantum Monte-Carlo simulations [77, 79, 81], the numerical renormalization group [82], the Lanczos method [83], and other techniques [79].

5.2 Characteristic features of the DMFT

In the DMFT the mean field is dynamical, whereby local quantum fluctuations are fully taken into account, but is spatially independent because of the infinitely many neighbors of every lattice site. The only approximation of the DMFT when applied in $d < \infty$ is the neglect of the $\boldsymbol{k}$-dependence of the self-energy ("single-site DMFT"). The DMFT provides a comprehensive, non-perturbative and thermodynamically consistent approximation scheme for the investigation of correlated lattice models at all interaction strengths. It describes fluctuating moments and the renormalization of quasiparticles and is especially valuable for the study of correlation problems at intermediate couplings.
The DMFT allows one to define electronic correlations in such a way that they can be tested experimentally, for example, by electron spectroscopies. Namely, correlations lead to transfer of spectral weight and to a finite lifetime of quasiparticles through the real and imaginary part of the dynamic self-energy, respectively. This is particularly useful for understanding and characterizing the correlation-induced metal-insulator transition.

5.2.1 The Mott-Hubbard metal-insulator transition

The correlation driven transition between a paramagnetic metal and a paramagnetic insulator, first discussed by Mott [84, 85] and now referred to as Mott- or Mott-Hubbard metal-insulator transition, is one of the most intriguing phenomena in condensed matter physics [86, 20]. This transition is a consequence of the quantum-mechanical competition between the kinetic energy of the electrons and their local interaction U. Namely, the kinetic energy prefers the electrons to be mobile (a wave effect) which leads to doubly occupied sites and thereby to interactions between the electrons (a particle effect). For large values of U the doubly occupied sites become energetically very costly. The system can reduce its total energy by localizing the electrons. Hence the Mott transition is a localization-delocalization transition [80]. While the Gutzwiller-

Brinkman-Rice approach [41] gives a good description of the quasiparticle behavior, it cannot reproduce the upper and lower Hubbard bands. Here the DMFT has been extremely valuable since it provided detailed insights into the nature of the Mott-Hubbard metal-insulator transition for all values of the interaction U and temperature T [79, 87, 80, 60].

5.2.2 Cold atoms in optical lattices

The investigation of correlation phenomena in cold atoms in optical lattices is a fascinating field of current research [28]. While the Hubbard model with its strictly local interaction is a strong approximation for electrons in solids, the model can describe cold atoms in optical lattices very accurately since the interaction between the atoms is indeed extremely short ranged. Here the DMFT has also been extremely useful. In fact, experiments with cold atoms in optical lattices have shown that the DMFT leads to reliable results even for finite-dimensional systems [88].

6 From models back to materials: DFT+DMFT

It took several decades to develop many-body techniques to study and understand at least the basic principles of the Hubbard model and the physics it describes. During that time first-principles investigations of correlated materials were out of reach. Electronic properties of solids were mainly studied within density-functional theory (DFT) [89, 90], e.g., in the local density approximation (LDA) [91], the generalized gradient approximation (GGA) [92], or using the so-called LDA+U method [93]. These approaches are able to describe the phase diagrams of many simple elements and semiconductors, and even of some insulators, quite accurately. Moreover, they often allow one to correctly predict the magnetic, orbital, and crystal structures of solids where the equilibrium structures are determined by the simultaneous optimization of the electron and lattice systems [94–96]. However, these methods usually fail to describe the correct electronic and structural properties of electronically correlated paramagnetic materials since they miss characteristic features of correlated electron systems, e.g., heavy quasiparticle behavior and Mott physics.

This changed dramatically with the advent of the DMFT. The computational scheme obtained by merging DFT with DMFT, now referred to as DFT+DMFT (or more explicitly as LDA+DMFT, GGA+DMFT, etc.), provides a powerful new method for the calculation of the electronic, magnetic, and structural properties of correlated materials from first principles [97–103]. The DFT+DMFT approach is able to describe and explain the effect of finite temperatures, including thermally driven phase transitions, in real materials. By overcoming the limitations of conventional band-structure methods, it opened up new vistas for fully microscopic investigations of the structural properties of strongly correlated systems, and has already led to many important insights into the properties of strongly correlated materials.

To illustrate the power of the DFT+DMFT approach and, at the same time, stay in line with the historically motivated discussion of correlated electron physics in section 1, I will limit the following presentation to elemental iron (Fe). Iron has been known for its extraordinary

magnetic and metallurgical properties for several thousand years already [2]. Since iron is the main constituent of the Earth's core it is also of great interest in geophysics [104].[23] More information about the DFT+DMFT approach can be found in the lecture notes of the Autumn Schools in 2011 and 2014 [25]. A detailed presentation will be given by E. Pavarini in her lecture during this Autumn School.

6.1 Metallic ferromagnetism

The Hubbard model had been introduced in 1963 in the attempt to explain ferromagnetism in $3d$ metals such as Fe, Co, and Ni [14–16]. But the resulting many-body problem turned out to be so hard to solve that it was uncertain for a long time whether the Hubbard model would be able to fulfill the expectations. Studies of the stability of ferromagnetism in the Hubbard model are made difficult not only by the fact that investigations have to be performed at intermediate coupling strengths, but also by the delicate dependence of the kinetic energy on the lattice structure, orbital overlap (determining the hopping amplitudes), and electronic density. It is well-known from Hartree-Fock-type approximations that the shape of the density of states of non-interacting electrons plays a very important role for ferromagnetism. Indeed, a peak at one of the band edges as in the case of the fcc-lattice is known to be favorable for ferromagnetism. This is supported by the observation that Co and Ni, having a non-bipartite hcp and fcc lattice structure, respectively, show a full magnetization, while bcc Fe is only partially magnetized (for a discussion with detailed references see Ref. [106]).

Investigations of the stability of metallic ferromagnetism on fcc-type lattices within DMFT were first performed by Ulmke [107]. For a generalized fcc lattice in $d = \infty$ and at an intermediate interaction strength of $U = 4$, he found ferromagnetic solutions around quarter filling ($n \simeq 0.5$), with the susceptibility χ_F obeying a Curie-Weiss law (Fig. 5). Below T_c the magnetization M grows rapidly, reaching more than 80% of the fully polarized value ($M_{max} = n = 0.58$) at the lowest temperature (30% below T_c). It is remarkable that the data points $M(T)$ in Fig. 5 are consistent with a Brillouin function (dashed curve) with the same critical temperature of $T_c = 0.05$ and an extrapolated full polarization at $T = 0$. So a Curie-Weiss-type static susceptibility with Brillouin-function-type magnetization, and a non-integer magneton number as in $3d$ transition metals are seen to coexist. These two features were usually thought to arise from seemingly contrasting physical effects: the former to localized spins, and the latter to itinerant electrons. However, these conclusions were derived from static mean-field-type approximations such as the Weiss mean-field theory for spin models and Hartree-Fock mean-field theory for electrons. Now we understand that these features appear naturally also in correlated electronic systems, where they are generated by the quantum dynamics of the many-electron problem. Within DMFT the seemingly paradoxical behavior of the magnetization and the susceptibility in band ferromagnets is resolved without difficulty.

[23] Iron is also vital for the human body, in particular in the production of blood. Many-body effects in the kernel of hemoglobin were recently found to be essential to explain the binding of CO and O_2 to heme [105].

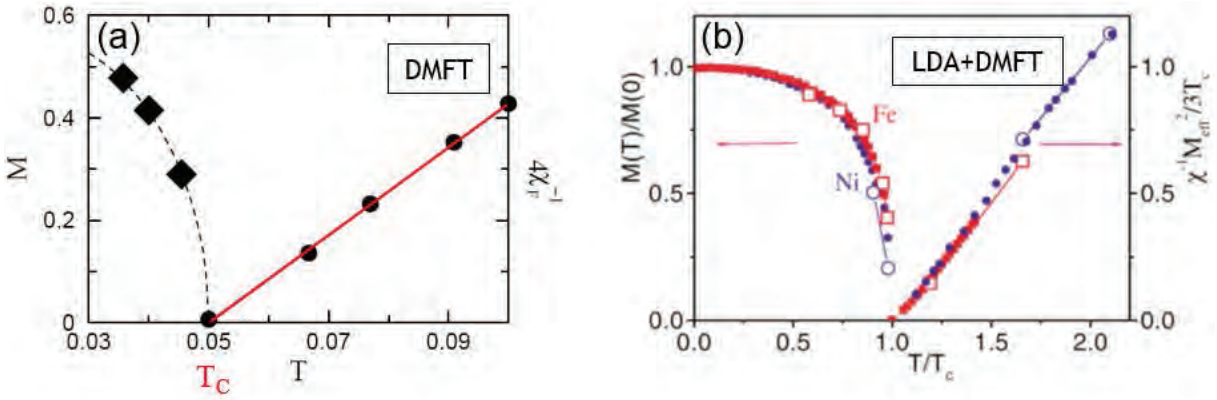

Fig. 5: *Magnetization and inverse ferromagnetic susceptibility calculated (a) by DMFT for the one-band Hubbard model on a generalized fcc lattice in $d = \infty$ at $U = 4$ and $n = 0.58$ (adapted from Ref. [107]), and (b) by LDA+DMFT for Fe (open squares) and Ni (open circles), where the results are compared with experimental results for Fe (squares) and Ni (circles); adapted from Ref. [108]). For details see text.*

Shortly thereafter Lichtenstein, Katsnelson and Kotliar [108] obtained the first finite-temperature results for the magnetic properties of elemental Fe and Ni within the *ab initio* LDA+DMFT approach. The temperature dependence of the magnetization and of the inverse ferromagnetic susceptibility of Fe and Ni explain the experimental data remarkably well.[24] The shape of the curves agrees with that obtained by Ulmke for the Hubbard model on fcc-type lattices within DMFT [107]. This demonstrates that the Hubbard model is indeed able to explain fundamental features of ferromagnetism in $3d$ metals such as Fe and Ni. Moreover the microscopic origin of the exchange couplings in ferromagnetic bcc Fe was recently clarified using the DFT+DMFT scheme [109].

The critical behavior of the magnetization and of the inverse susceptibility observed in Refs. [107, 108] is clearly mean-field-like. Since the DMFT is derived from the Hubbard model in the limit $d = \infty$ this does not come unexpected. Deviations from mean-field exponents will be due to non-local effects which go beyond single-site DMFT. The critical properties of the Hubbard model will be discussed in the lecture by K. Held during this Autumn School.

[24] The temperature scale is in units of T/T_C. The actual Curie temperatures T_C for Fe(Ni) were obtained as $1900(700)$ K [108] and are in reasonable agreement with the experimental values $1043(631)$ K. The fact that the calculated values are higher than the experimental values is not surprising since the single-site nature of the DMFT cannot capture the reduction of T_C due to spin waves with finite wavelengths.

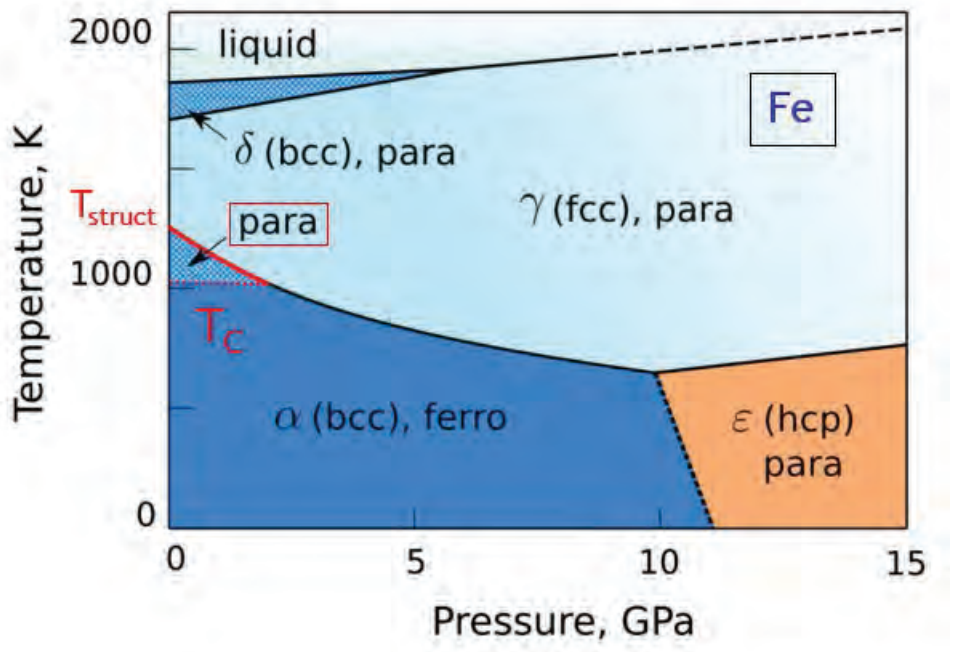

Fig. 6: *Schematic temperature-pressure (T-p) phase diagram of iron; adapted from Ref. [110].*

6.2 Electronic correlations and lattice stability of solids: paramagnetic Fe

Iron exhibits a rich phase diagram with at least four allotropic forms (Fig. 6). At ambient conditions iron is ferromagnetic and has a bcc crystal structure (α phase). Upon heating above the Curie temperature $T_C \sim 1043$ K, α iron becomes paramagnetic, but remains in its bcc crystal structure. Only when the temperature is increased above $T_{\text{struct}} \sim 1185$ K does α iron exhibit a structural phase transition to a fcc structure (γ phase). Clearly iron is a complicated material where magnetic order and correlation effects play an important role; for a discussion see [111, 112]. In spite of intensive research on iron its electronic and lattice properties are still not sufficiently understood.

6.2.1 Lattice stability and phonon spectra near the α-to-γ transition

State-of-the-art band structure methods provide a qualitatively correct description of various electronic and structural properties of iron [113]. For example, these methods provide a good quantitative understanding of the equilibrium crystal structure and the lattice dynamical properties of the ferromagnetic α phase. However, applications of these techniques to describe, for example, the α-to-γ phase transition in iron, do not lead to satisfactory results. They predict a simultaneous transition of the structure and the magnetic state at the bcc-to-fcc phase transition while, in fact, the bcc-to-fcc phase transition occurs only about 150 K above T_C. Moreover, the elastic and dynamical stability of the bcc phase is found to depend sensitively on the value of the magnetization. For example, in the absence of a magnetization, standard band-structure methods predict bcc iron to be unstable [114]. We now understand that the stability of paramagnetic bcc iron is due to the presence of local moments above T_C which cannot be treated realistically by conventional band-structure techniques.

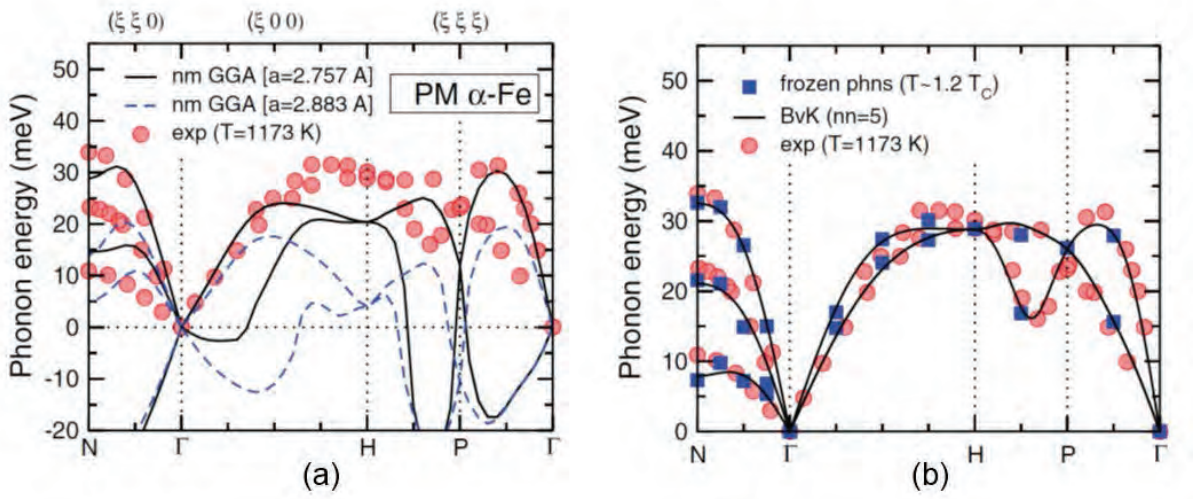

Fig. 7: *Phonon dispersion curves and corresponding phonon density of states of paramagnetic bcc Fe as calculated within (a) the non-magnetic GGA and (b) GGA+DMFT. The results are compared with neutron inelastic scattering measurements at 1173 K; adapted from Ref. [117].*

This problem has been overcome by employing the DFT+DMFT approach which allows one to study correlated materials both in the long-range ordered and the paramagnetic state [115–118, 110, 111]. The DFT+DMFT method naturally accounts for the existence of local moments above T_C and provides a good quantitative description of the properties of α iron. In particular, DFT+DMFT studies of the equilibrium crystal structure and phase stability of iron at the α-to-γ phase transition found that the bcc-to-fcc phase transition indeed takes place at a temperature well above the magnetic transition, at about 1.3 T_C, in agreement with experiment [110].

In view of the crucial importance of electronic correlations for the phase stability of α iron Leonov *et al.* [117] also computed the phonon dispersion relations of paramagnetic iron near the bcc-to-fcc phase transition (Fig. 7). For this purpose the DFT+DMFT approach implemented with the frozen-phonon method was employed [117]. To evaluate the phonon frequencies for arbitrary wave vectors in the Brillouin zone, lattice dynamical calculations were performed on the basis of a Born-von Kármán model with interactions expanded up to the 5-th nearest-neighbor shell. The calculated phonon dispersions of the bcc phase of iron show the typical behavior of a bcc metal with an effective Debye temperature ~ 458 K. The phonon frequencies are overall positive, implying mechanical stability of the bcc lattice structure at $\sim 1.2\ T_C$, i.e., well above the Curie temperature, in agreement with experiment. This corrects the results obtained with the non-magnetic GGA which finds the bcc lattice to be dynamically unstable even for the equilibrium lattice constant $a = 2.883$ Å. These results clearly demonstrate the crucial importance of electronic correlations for an explanation of the thermodynamic and the lattice dynamical stability of the paramagnetic bcc phase of iron [117]. Overall, the structural phase stability, equilibrium lattice constant, and phonon frequencies of bcc iron obtained by DFT+DMFT are in remarkably good agreement with the experimental data which were taken at nearly the same reduced temperature T/T_C [119]. Results obtained for the lattice stability of Fe at even higher temperatures are discussed in Refs. [117, 111].

7 Conclusions and outlook

By now the dynamical mean-field theory (DMFT) has developed into a versatile method for the investigation of electronic systems with strong correlations. It provides a comprehensive, non-perturbative and thermodynamically consistent approximation scheme for the investigation of finite-dimensional systems, in particular for dimension $d = 3$, and is particularly useful for the study of problems where perturbative approaches fail. For this reason the DMFT has now become the standard mean-field theory for fermionic correlation problems. The generalization of this approach and its applications is currently a subject of active research. Non-local extensions of the DMFT play a particularly important role [120, 81, 121]; see also the lecture by H. Hafermann during this Autumn School. They make it possible to study and explain correlation effects which occur on the scale of several lattice constants. Furthermore, investigations of inhomogeneous bulk systems and of internal and external inhomogeneities, such as surfaces and interfaces [122–127], lead to an improved understanding of correlation effects in thin films and multi-layered nanostructures. This is particularly desirable in view of the novel functionalities of these structures and their possible applications in electronic devices.

The study of correlated electrons out of equilibrium using the DMFT has become yet another fascinating new research area. Non-equilibrium DMFT is able to explain, and even predict, the results of time-resolved experiments [128] and will be discussed in the lecture by M. Eckstein during this Autumn School.

In particular, the combination of the DMFT with methods for the computation of electronic band structures ("DFT+DMFT") has led to a conceptually new theoretical framework for the realistic study of correlated materials.

The development of a comprehensive theoretical approach which allows for a quantitative understanding and prediction of correlation effects in materials, ranging from complex inorganic materials all the way to biological systems, is one of the great challenges for modern theoretical physics. The lecture notes of the "Autumn Schools on Correlated Electrons" held at the Forschungszentrum Jülich since 2011 provide an excellent introduction into this very active field of research [25].

References

[1] J.C. Maxwell, Phil. Mag. **90**, 11 (1861)

[2] D.C. Mattis: *The Theory of Magnetism I: Statics and Dynamics* (Springer, Berlin, 1988)

[3] P. Weiss, Comptes Rendus **143**, 1136 (1906)

[4] E. Ising, Z. Phys. **31**, 253 (1925)

[5] W. Heisenberg, Z. Phys. **49**, 619 (1928)

[6] F. Bloch, Z. Phys. **57**, 545 (1929)

[7] L. Hoddeson, G. Baym, and M. Eckert, Rev. Mod. Phys. **59**, 287 (1987)

[8] J.C. Slater, Phys. Rev. **49**, 537 (1936)

[9] E. Wigner, Phys. Rev. **46**, 1002 (1934)

[10] D. Pines: *The Many-Body Problem* (W.A. Benjamin, Reading, 1962)

[11] J.C. Slater, Rev. Mod. Phys. **25**, 199 (1953)

[12] E.P. Wohlfarth, Rev. Mod. Phys. **25**, 211 (1953)

[13] J.H. Van Vleck, Rev. Mod. Phys. **25**, 220 (1953)

[14] M.C. Gutzwiller, Phys. Rev. Lett. **10**, 159 (1963)

[15] J. Hubbard, Proc. Roy. Soc. London A **276**, 238 (1963)

[16] J. Kanamori, Prog. Theor. Phys. **30**, 275 (1963)

[17] N. Grewe and F. Steglich, in K.A. Gschneidner Jr. and L. Eyring (eds.): *Handbook on the Physics and Chemistry of Rare Earths*, Vol. 14 (North Holland, Amsterdam, 1991) p. 343

[18] J.R. Schrieffer (ed.): *Handbook of High-Temperature Superconductivity* (Springer, Berlin, 2007)

[19] E. Dagotto: *Nanoscale Phase Separation and Colossal Magnetoresistance* (Springer, Berlin, 2002)

[20] M. Imada, A. Fujimori, and Y. Tokura, Rev. Mod. Phys. **70**, 1039 (1998)

[21] H. v. Löhneysen, A. Rosch, M. Vojta, and P. Wölfle, Rev. Mod. Phys. **79**, 1015 (2007)

[22] Y. Tokura, Physics Today, July 2003, p. 50

[23] P. Fulde: *Electron Correlations in Molecules and Solids* (Springer, Berlin, 2002)

[24] P. Fazekas: *Lecture Notes on Electron Correlation and Magnetism* (World Scientific, Singapore, 1999)

[25] The "Lecture Notes of the Autumn Schools on Correlated Electrons" which have been edited by E. Pavarini, E. Koch and various co-editors since 2011 provide comprehensive and up-to-date information about electronic correlations in models and materials and about theoretical techniques for their investigation: `https://www.cond-mat.de/events/correl.html`

[26] A. Montorsi (ed.): *The Hubbard Model — A Reprint Volume* (World Scientific, Singapore, 1992)

[27] D. Jaksch, C. Bruder, J.I. Cirac, C.W. Gardiner, and P. Zoller, Phys. Rev. Lett. **81**, 3108 (1998)

[28] I. Bloch, J. Dalibard, and W. Zwerger, Rev. Mod. Phys. **80**, 885 (2008)

[29] E. Lieb and F.Y. Wu, Phys. Rev. Lett. **20**, 1445 (1968)

[30] R. Peierls, Contemp. Physics **21**, 3 (1980)

[31] R.J. Baxter: *Exactly Solved Models in Statistical Mechanics* (Academic Press, London, 1982)

[32] R. Brout, *Phys. Rev.* **118**, 1009 (1960)

[33] M.E. Fisher and D.S. Gaunt, Phys. Rev. **133**, A224 (1964)

[34] C.J. Thompson, *Commun. Math. Phys.* **36**, 255 (1974)

[35] C. Itzykson and J.-M. Drouffe: *Statistical Field Theory* (Cambridge University Press, Cambridge, 1989)

[36] W. Langer, M. Plischke, and Mattis, Phys. Rev. Lett. **23**, 1448 (1969)

[37] K. Dichtel, R.J. Jelitto, and H. Koppe, Z. Phys. **246**, 248 (1971)

[38] U. Wolff, Nucl. Phys. B **225**, 391 (1983)

[39] J. Bardeen, L.N. Cooper and J.R. Schrieffer; Phys. Rev. **108**, 1175 (1957); E. Feenberg: *Theory of Quantum Fluids* (Academic, New York, 1969); R.P. Feynman: *Statistical Physics* (Benjamin, Reading, 1972); C.M. Varma and Y. Yafet, Phys. Rev. B **13**, 2950 (1976); V.R. Pandharipande and R.B. Wiringa, Rev. Mod. Phys. **51**, 821 (1979); R.B. Laughlin, Phys. Rev. Lett. **50**, 1395 (1983); O. Gunnarsson and K. Schönhammer, Phys. Rev. B **28**, 4315 (1983); P.W. Anderson, P.A. Lee, M. Randeria, T.M. Rice, N. Trivedi, and F.C. Zhang, J. Phys.: Condens. Matter **16** R755–R769 (2004)

[40] M.C. Gutzwiller, Phys. Rev. **137**, A1726 (1965)

[41] D. Vollhardt, Rev. Mod. Phys. **56**, 99 (1984)

[42] P.G.J. van Dongen and D. Vollhardt, Phys. Rev. B **40**, 7252 (1989)

[43] W.F. Brinkman and T.M. Rice, Phys. Rev. B **2**, 4302 (1970)

[44] J. Hubbard, Proc. Roy. Soc. London A **281**, 401 (1964)

[45] R.J. Elliott, J.A. Krumhansl, and P.L. Leath, Rev. Mod. Phys. **46**, 465 (1974)

[46] P.W. Anderson and W.F. Brinkman, in K.H. Bennemann and J.B. Ketterson (eds.): *The Physics of Liquid and Solid Helium*, Part II (Wiley, New York, 1978), p. 177

[47] D. Vollhardt: *From Gutzwiller Wave Functions to Dynamical Mean-Field Theory*, in E. Pavarini, E. Koch, D. Vollhardt, A. Lichtenstein (eds.): *DMFT at 25: Infinite Dimensions*, Modeling and Simulation, Vol. 4 (Forschungszentrum Jülich, 2014) https://www.cond-mat.de/events/correl14/manuscripts/vollhardt.pdf

[48] D. Vollhardt, P. Wölfle, and P.W. Anderson, Phys. Rev. B **35**, 6703 (1987)

[49] G. Kotliar and A.E. Ruckenstein, Phys. Rev. Lett. **57**, 1362 (1986)

[50] For an account by Andrei Ruckenstein of the developments leading to the formulation of the Kotliar-Ruckenstein slave-boson MFT see https://www.aspenphys.org/aboutus/history/presidentialessays/ruckenstein.html

[51] W. Metzner and D. Vollhardt, Phys. Rev. Lett. **59**, 121 (1987)

[52] W. Metzner and D. Vollhardt, Phys. Rev. B **37**, 7382 (1988); Erratum: Phys. Rev. B **39**, 12339 (1989)

[53] F. Gebhard, and D. Vollhardt, Phys. Rev. Lett. **59**, 1472 (1987)

[54] F. Gebhard and D. Vollhardt, Phys. Rev. B **38**, 6911 (1988)

[55] F.D.M. Haldane, Phys. Rev. Lett. **60**, 635 (1988)

[56] B.S. Shastry, Phys. Rev. Lett. **60**, 639 (1988)

[57] W. Metzner and D. Vollhardt, Phys. Rev. Lett. **62**, 324 (1989)

[58] W. Metzner, Z. Phys. B **77**, 253 (1989)

[59] P.G.J. van Dongen, F. Gebhard, and D. Vollhardt, Z. Phys. **76**, 199 (1989)

[60] D. Vollhardt, in A. Avella and F. Mancini (eds.): *Lectures on the Physics of Strongly Correlated Systems XIV*, *AIP Conference Proceedings*, Vol. 1297 (American Institute of Physics, Melville, 2010) p. 339; http://arxiv.org/abs/1004.5069v3

[61] F. Gebhard, Phys. Rev. B **41**, 9452 (1990)

[62] J. Bünemann, F. Gebhard, and W. Weber, Found. of Physics **30**, 2011 (2000)

[63] T. Schickling, J. Bünemann, F. Gebhard, and W. Weber, New J. Phys. **16**, 93034 (2014)

[64] K. Byczuk and D. Vollhardt, Phys. Rev. **B 77**, 235106 (2008)

[65] E. Müller-Hartmann, Z. Phys. B **74**, 507 (1989)

[66] E. Müller-Hartmann, Z. Phys. B **76**, 211 (1989)

[67] V. Janiš, Z. Phys. B **83**, 227 (1991)

[68] V. Janiš and D. Vollhardt, Int. J. Mod. Phys. **B6**, 731 (1992)

[69] R. Vlaming and D. Vollhardt, Phys. Rev. **B 45**, 4637 (1992)

[70] V. Janiš and D. Vollhardt, Phys. Rev. **B 46**, 15712 (1992)

[71] H. Schweitzer and G. Czycholl, Solid State Comm. **69**, 171 (1989)

[72] U. Brandt and C. Mielsch, Z. Phys. B **75**, 365 (1989)

[73] P.G.J. van Dongen and D. Vollhardt, Phys. Rev. Lett. **65**, 1663 (1990)

[74] J.M. Luttinger and J.C. Ward, *Phys. Rev.* **118**, 1417 (1960)

[75] A.C. Hewson: *The Kondo Problem to Heavy Fermions*
(Cambridge University Press, Cambridge, 1997)

[76] A. Georges and G. Kotliar, Phys. Rev. B **45**, 6479 (1992)

[77] M. Jarrell, Phys. Rev. Lett. **69**, 168 (1992)

[78] J.E. Hirsch and R.M. Fye, Phys. Rev. Lett. **56**, 2521 (1986)

[79] A. Georges, G. Kotliar, W. Krauth, and M.J. Rozenberg, Rev. Mod. Phys. **68**, 13 (1996)

[80] G. Kotliar and D. Vollhardt, Phys. Today **57**, 53 (2004)

[81] E. Gull, A.J. Millis, A.I. Lichtenstein, A.N. Rubtsov, M. Troyer, P. Werner,
Rev. Mod. Phys. **83**, 349 (2011)

[82] R. Bulla, T.A. Costi, and Th. Pruschke, Rev. Mod. Phys. **80**, 395 (2008)

[83] E. Koch: *The Lanczos Method*, in
E. Pavarini, E. Koch, D. Vollhardt, and A.I. Lichtenstein (eds.)
The LDA+DMFT approach to strongly correlated materials
Modeling and Simulation, Vol. 1 (Forschungszentrum Jülich, 2011)

[84] N.F. Mott, Rev. Mod. Phys. **40**, 677 (1968)

[85] N.F. Mott: *Metal–Insulator Transitions* (Taylor and Francis, London, 1990), 2nd edition

[86] F. Gebhard: *The Mott Metal-Insulator Transition* (Springer, Berlin, 1997)

[87] N. Blümer: *Metal-Insulator Transition and Optical Conductivity in High Dimensions* (Shaker Verlag, Aachen, 2003)

[88] U. Schneider, L. Hackermüller, S. Will, Th. Best, I. Bloch, T.A. Costi, R.W. Helmes, D. Rasch, A. Rosch, Science **322**, 1520 (2008)

[89] P. Hohenberg and W. Kohn, Phys. Rev. B **136**, 864 (1964)

[90] W. Kohn and L.J. Sham, Phys. Rev. **140**, A1133 (1965)

[91] R.O. Jones, O. Gunnarsson, Rev. Mod. Phys. **61**, 689 (1989)

[92] J.P. Perdew, K. Burke, M. Ernzerhof, Phys. Rev. Lett. **77**, 3865 (1996)

[93] V.I. Anisimov, J. Zaanen, O.K. Andersen, Phys. Rev. B **44**, 943 (1991)

[94] S. Baroni, S. de Gironcoli, A.D. Corso, P. Giannozzi, Rev. Mod. Phys. **73**, 515 (2001)

[95] P. Blaha, K. Schwarz, G. Madsen, D. Kvasnicka, J. Luitz: *WIEN2k, An Augmented Plane Wave + Local Orbitals Program for Calculating Crystal Properties*. (Karlheinz Schwarz, TU Wien, 2001)

[96] G. Kresse, J. Hafner, Phys. Rev. B **47**, 558 (1993)

[97] V.I. Anisimov, A.I. Poteryaev, M.A. Korotin, A.O. Anokhin, G. Kotliar, J. Phys.: Condens. Matt. **9**, 7359 (1997)

[98] A.I. Lichtenstein, M.I. Katsnelson, Phys. Rev. B **57**, 6884 (1998)

[99] K. Held, I.A. Nekrasov, G. Keller, V. Eyert, N. Blümer, A.K. McMahan, R.T. Scalettar, T. Pruschke, V.I. Anisimov, and D. Vollhardt, Psi-k Newsletter **56**, 65 (2003); reprinted in Phys. Status Solidi B **243**, 2599 (2006)

[100] G. Kotliar, S.Y. Savrasov, K. Haule, V.S. Oudovenko, O. Parcollet, C.A. Marianetti, Rev. Mod. Phys. **78**, 865 (2006)

[101] K. Held, Adv. Phys. **56**, 829 (2007)

[102] M.I. Katsnelson, V. Yu. Irkhin, L. Chioncel, A.I. Lichtenstein, and R.A. de Groot, Rev. Mod. Phys. **80**, 315 (2008)

[103] D. Vollhardt and A.I. Lichtenstein (eds.): *Dynamical Mean-Field Approach with Predictive Power for Strongly Correlated Materials* Eur. Phys. J. Spec. Top. **226** (2017)

[104] S. Tateno, K. Hirose, Y. Ohishi, Y. Tatsumi, Science **330**, 359 (2013); A. Hausoel, M. Karolak, E. Şaşıoğlu, A. Lichtenstein, K. Held, A. Katanin, A. Toschi, G. Sangiovanni, Nature Comm. **8**, 16062 (2017)

[105] C. Weber, D.D. O'Regan, N.D.M. Hine, P.B. Littlewood, G. Kotliar, M.C. Payne, Phys. Rev. Lett. **110**, 106402 (2013)

[106] D. Vollhardt, N. Blümer, K. Held, M. Kollar, J. Schlipf, M. Ulmke: Z. Phys. B **103**, 283 (1997); D. Vollhardt, N. Blümer, K. Held, M. Kollar, J. Schlipf, M. Ulmke, J. Wahle: *Advances In Solid State Physics 38*, p. 383 (Vieweg, Wiesbaden 1999)

[107] M. Ulmke: Euro. Phys. J. B **1**, 301 (1998)

[108] A.I. Lichtenstein, M.I. Katsnelson, G. Kotliar, Phys. Rev. Lett. **87**, 067205 (2001)

[109] Y.O. Kvashnin, R. Cardias, A. Szilva, I. Di Marco, M.I. Katsnelson, A.I. Lichtenstein, L. Nordström, A.B. Klautau, O. Eriksson, Phys. Rev. Lett. **116**, 217202 (2016)

[110] I. Leonov, A.I. Poteryaev, V.I. Anisimov, D. Vollhardt, Phys. Rev. Lett. **106**, 106405 (2011)

[111] I. Leonov, A.I. Poteryaev, Y.N. Gornostyrev, A.I. Lichtenstein, M.I. Katsnelson, V.I. Anisimov, D. Vollhardt, Sci. Rep. **4**, 5585 (2014)

[112] J. Kuneš, I. Leonov, P. Augustinský, V. Křápek, M. Kollar, and D. Vollhardt, Eur. Phys. J. Spec. Top. **226**, 2641 (2017)

[113] D.J. Singh, W.E. Pickett, H. Krakauer, Phys. Rev. B **43**, 11628 (1991); S.V. Okatov, A.R. Kuznetsov, Y.N. Gornostyrev, V.N. Urtsev, M.I. Katsnelson, Phys. Rev. B **79**, 094111 (2009); F. Körmann, A. Dick, B. Grabowski, T. Hickel, J. Neugebauer, Phys. Rev. B **85**, 125104 (2012)

[114] H.C. Hsueh, J. Crain, G.Y. Guo, H.Y. Chen, C.C. Lee, K.P. Chang, and H.L. Shih, Phys. Rev. B **66**, 052420 (2002)

[115] A.I. Lichtenstein, M.I. Katsnelson, and G. Kotliar, Phys. Rev. Lett. **87**, 067205 (2001)

[116] A.A. Katanin, A.I. Poteryaev, A.V. Efremov, A.O. Shorikov, S.L. Skornyakov, M.A. Korotin, V.I. Anisimov, Phys. Rev. B **81**, 045117 (2010)

[117] I. Leonov, A.I. Poteryaev, V.I. Anisimov, D. Vollhardt, Phys. Rev. B **85**, R020401 (2012)

[118] L.V. Pourovskii, J. Mravlje, M. Ferrero, O. Parcollet, I.A. Abrikosov, Phys. Rev. B **90**, 155120 (2014)

[119] J. Neuhaus, W. Petry, A. Krimmel, Physica B **234-236**, 897 (1997)

[120] Th. Maier, M. Jarrell, Th. Pruschke, and M.H. Hettler, Rev. Mod. Phys. **77**, 1027 (2005)

[121] K. Held: *Dynamical Vertex Approximation*, in
E. Pavarini, E. Koch, D. Vollhardt, A. Lichtenstein (eds.):
DMFT at 25: Infinite Dimensions Modeling and Simulation, Vol. 4
(Forschungszentrum Jülich, 2014)

[122] M. Potthoff and W. Nolting, Phys. Rev. B **59**, 2549 (1999)

[123] R.W. Helmes, T.A. Costi, and A. Rosch, Phys. Rev. Lett. **100**, 056403 (2008)

[124] M.J. Han, X. Wang, C.A. Marianetti, and A.J. Millis, Phys. Rev. Lett. **107**, 206804 (2011)

[125] J.K. Freericks, *Transport in multilayered nanostructures — The dynamical mean-field approach*, 2nd edition (Imperial College Press, London, 2016)

[126] T. Yoshida and N. Kawakami, Phys. Rev. B **95**, 045127 (2017)

[127] I. Di Marco, A. Held, S. Keshavarz, Y.O. Kvashnin, and L. Chioncel,
Phys. Rev. B **97**, 035105 (2018)

[128] H. Aoki, N. Tsuji, M. Eckstein, M. Kollar, T. Oka, and P. Werner,
Rev. Mod. Phys. **86**, 779 (2014)